Passive Bipedal Running

T. McGeer

Proceedings of the Royal Society of London. Series B, Biological Sciences, Vol. 240, No. 1297 (May 22, 1990), 107-134.

Stable URL:
http://links.jstor.org/sici?sici=0080-4649%2819900522%29240%3A1297%3C107%3APBR%3E2.0.CO%3B2-Q

Proc. R. Soc. Lond. B **240**, 107–134 (1990)
Printed in Great Britain

Passive bipedal running

By T. McGeer

School of Engineering Science, Simon Fraser University, Burnaby, British Columbia, Canada V5A 1S6

(*Communicated by R. M. Alexander, F.R.S. – Received* 11 *October* 1989 – *Revised* 19 *January* 1990)

Human-like running is a natural dynamic mode of a simple mechanical biped. Such a machine consists of two telescoping legs with linear springs, connected by a hip joint with a torsional spring. It will run passively; no pattern of forcing is required to generate the gait. With careful design its energy consumption can approach zero, but in any case the passive cycle can be 'pumped' by various means to sustain running over a range of speeds and slopes. Passive running can also be realized over a wide range of mechanical design parameters. Some parameter sets produce cycles that are inherently stable; otherwise the mode can be actively stabilized by a simple control law. Thus the passive running model offers an effective foundation for design of practical running machines, and also provides an insight into the physics of human locomotion.

Symbols used in the text

(*Numbers in parentheses denote the relevant defining equations*)

Italic

A_f	frontal area
c	nominal foot → leg CM distance (figure 1)
c_T	hip → torso CM distance (14)
C_D	aerodynamic drag coefficient (10)
d	viscous damping coefficient (17), (40)
E	energy
F	force
g	gravitational acceleration (figure 1)
I	moment of inertia (34), (35), (45), (46), (47), (48), (49)
K	spring constant (figure 1)
l	leg length (figure 1)
l_0	nominal leg length (figure 1)
l_{zf}	relaxed leg length (16)
l_0'	stance thrust coefficient (16)
m	mass (figure 1)
R	foot radius (figure 1)
$\vec{r}_{HC}$	hip → stance leg CM vector (31)
$\vec{r}_{HF}$	hip → swing leg CM vector (32)
$\vec{r}_{PH}$	contact point → hip vector (33)
r_{gyr}	radius of gyration
$\vec{S}$	stride function (1)
$\nabla\vec{S}$	gradient of $\vec{S}$ (2)
s	take-off → take-off translation
SR	specific resistance (7)
T	torque
T_T	stance/torso torque (13)
V	linear velocity
v_o	bounce parameter (26)
w	leg axis → mass centre offset (figure 1)
$\hat{x}_C$	unit vector along the stance leg (29)
$\hat{y}_C$	unit vector normal to the stance leg
z	eigenvalue of $\nabla\vec{S}$ (6)

Greek

γ	slope, positive downhill (figure 1)	θ	angle relative to surface normal (figure 1)
γ_g	slope for gravity-powered running	ρ	air density
$\Delta\theta$	change from steady-cycle θ (6)	τ	dimensionless time $\sqrt{l_0/g}$
$\Delta\Omega$	change from steady-cycle Ω (6)	Ω	angular speed
$\Delta\dot{l}_{C_T}$	change from steady-cycle $\dot{l}_{C_T}$ (6)	ω_l	leg-compression frequency
Δl_{eq}	change in equilibrium from l_0 (24)	ω_l'	leg-compression frequency modified by centrifugal effect (23)
ζ	damping ratio (42)	ω_{sc}	scissor frequency

Sub- and superscripts

0	steady-cycle conditions	k	step index
b	flight phase	T	take-off, torso
C	stance leg	x	normal to the ground (figure 1)
c	stance phase	y	along the ground (figure 1)
CM	biped's mass centre	+	immediately after landing
F	swing leg	−	immediately before landing
g	due to gravity		

1. Passive dynamics in bipedal locomotion

Today we can build machines to travel beyond the outer planets, yet we do not really understand how we move about on our own two legs. Would that we knew more; we might then improve athletic performance, effectively rehabilitate the handicapped, and design rough-terrain vehicles with horse- or human-like mobility. But there arises a central problem: whereas spacecraft (and most other vehicles) can simply drone through time in steady state, legged devices locomote only via an elaborate pattern of motion. At first glance this seems to call for a corresponding pattern of control. Hence many students of animal locomotion try to elucidate underlying neuromuscular activity, and designers of legged machines introduce multiple actuating devices and devise suitable algorithms for controlling them. (Various references on algorithm design are given by McGeer (1990*a*).) It turns out, however, that legged locomotion need not call for any control at all. In fact, just as a pendulum will swing by itself, so a simple mechanism, two straight legs connected by a pin joint, will walk by itself in a quite human-like style. McGeer (1990*a*) reported analytical and experimental studies of this 'passive dynamic walking' effect. Here I report an analogous effect for running.

Of course, the practical advantage of running over walking is higher speed; let us note the essential physics that makes higher speed possible. Walking and running are distinguished formally by the height of the mass centre at midstance (McMahon *et al.* 1987). In walking, midstance is the instant of maximum height, as the hip rotates over a rigidly extended stance leg. Alexander (1983) noted that centrifugal effect on this trajectory lightens the contact force at the foot; as the speed approaches $\sqrt{gl_0}$ the force goes to zero and further acceleration is precluded. (You will feel this effect if you try to walk unusually fast.) To go faster you must diminish centrifugal effect by shortening the leg through midstance; we call this new gait a run, with midstance the instant of minimum height. Normally the

subsequent extension is sufficiently vigorous to cause lift-off, which produces a flight phase after each stance period.

In §§2 and 3 I describe a simple mechanism that runs, and note salient features of its motion. Next I introduce analytical methods for calculating its gait and stability. These methods are then used to evaluate energy dissipation, means for recouping energy losses, and robustness of running behaviour with respect to variations in model parameters.

2. The model

Figure 1 shows the biped runner. It has semicircular feet, straight legs, and a point mass at the hip. (McGeer (1988) has shown that the hip mass has roughly the same effects as an extended torso.) Each leg has a translational spring parallel to its axis, which allows for compression during stance, and the subsequent rebound into the flight phase. The hip has a torsional spring, which moves the legs back and forth in a 'scissor' action. All motion is confined to the plane of the figure. The feet are massless, so that all of the machine's mass is above the leg springs. The legs themselves have arbitrary mass and inertia. All of the dynamics analysis is done in dimensionless terms, with total mass m, nominal leg length l_0, and gravity g providing the base units. (One unit of time is therefore $\sqrt{l_0/g}$, one unit of inertia ml_0^2, one unit of stance spring stiffness mg/l_0, etc.)

For purposes of analysis, the mechanism of figure 1 need be complicated no further. However, practical running would call for one addition. When a biped

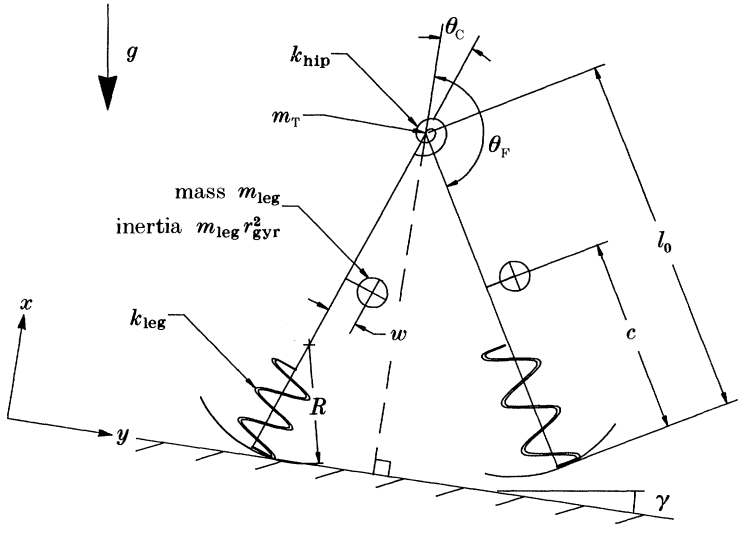

Figure 1. Running is a passive dynamic mode of this simple biped. The legs have arbitrary mass, centroid, and moment of inertia, and compress telescopically against linear springs. A torso is roughly approximated by a point mass at the hip. The feet are massless rigid semicircles. While running, the legs bounce between flight and stance phases, and are cycled back and forth in a scissor motion by a torsional spring at the hip. Note that angles are measured from the surface normal rather than the vertical.

recovers its free leg in preparation for the next stride, it must lift the foot clear of the ground to avoid toe stubbing. Thus humans flex the swing knee. In fact this may be a passive motion; Mochon & McMahon (1980) and McGeer (1990*b*) have shown that, at least in walking, a knee-jointed leg will flex and re-extend naturally during its recovery phase. Passive knee flexure might also work for running, but alternatively the free leg could be shortened by active means. In any case leg shortening would leave the motion of the basic straight-legged model essentially undisturbed.

3. The cycle

Figure 2 shows an example of running by our mechanical biped. (For the sake of interest we have chosen model parameters to match the speed and flight/stance times of a set of human data measured by McMahon *et al.* (1987).) The mathematics underlying figure 2 are explained in §4, but the motion can be understood without any calculations. In essence it is just a scissor oscillation proceeding in phase with vertical bouncing. During flight the hip spring first brakes spreading of the legs, and then starts to bring them back together; meanwhile the machine as a whole follows a ballistic arc, and rotates slightly so that the forward leg is first to strike the ground. Then during contact the legs cross while the overall mass centre bounces on the stance spring. Finally the machine takes off again when the contact force goes to zero. Initial conditions are then as they were for the previous stride, so the cycle repeats indefinitely (with the legs exchanging roles on alternate strides).

A quantitative look at cadence in this cycle reveals the central role of the hip-spring's scissor motion in generating the gait. The time for two strides of figure 2 (i.e. one full back-and-forth cycle for each leg) is $2.52\sqrt{l_0/g}$. By comparison, if the legs were allowed to scissor free in space, the inertia/spring period would be almost the same, namely $2.57\sqrt{l_0/g}$ (41). Similarly close correspondence is found over a wide range of speeds, stride lengths, and other model parameters (e.g. figure 4). Moreover the essential idea of 'bounce-and-scissor' locomotion extends beyond our bipedal model; Thompson & Raibert (1989) have shown similar cycles in monopeds. In the monopedal model the scissor action is between the leg and a relatively high-inertia torso.

These simple 'bounce-and-scissor' models could be adopted directly for design of mechanical runners. But what about for understanding natural locomotion? Obviously locomotion in nature is more complicated, but we believe that the physics is nevertheless likely to be similar. In walking we have investigated models ranging from something as simple as a gravity-powered rimless wagon wheel, through two-dimensional bipeds with knees (McGeer 1990*b*), torsos, and various methods of energy supply (McGeer 1988), to three-dimensional bipeds and quadrupeds (McGeer 1990*a*) whose passive cycles include a sideways rocking motion. The motions of these various models differ in detail, but not in their main features. (In particular, energy requirements, cadences, and link trajectories are generally similar from one model to the next.) Hence to study walking it is most sensible to begin with the simpler models, which demonstrate the essential physics

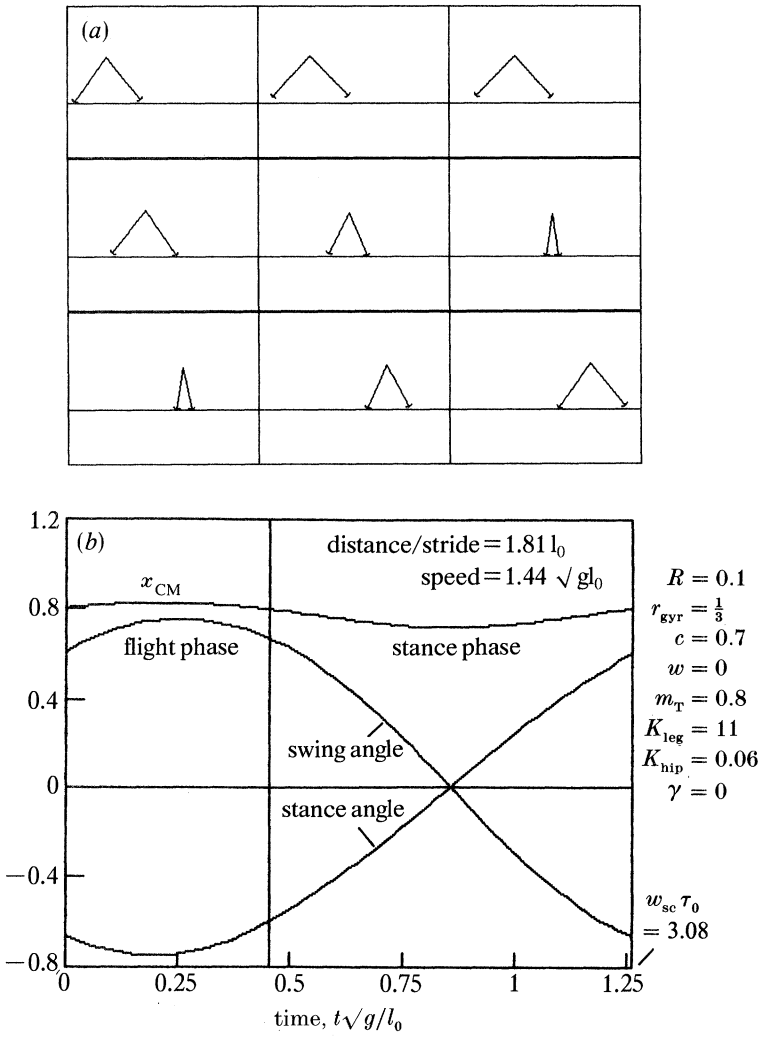

FIGURE 2. This example of a passive running cycle corresponds roughly to relaxed jogging in a human. All quantities are dimensionless; total mass m, nominal leg length l_0, and gravity g provide the base units. During flight the legs first spread and then return under the influence of the hip spring; meanwhile the overall mass centre follows a parabolic free fall (frames 1–4 of (*a*)). Then landing compresses the stance leg, and the swing leg is shortened as necessary to keep its foot clear (frames 5–8). Stance rebound throws the machine back off the ground, and the cycle then repeats with the legs exchanging roles. Note that no energy is dissipated during the cycle; it is simply exchanged between kinetic, gravitational, and elastic stores.

in the most uncomplicated form, and then add a sequence of complicating effects in pursuit of practicality and fidelity to natural behaviour.

In my view, the similar sequence for the study of running begins with the bouncing models of McMahon *et al.* (1987), which address the relation between stance leg stiffness, cadence and speed. The model considered here then integrates

this bouncing motion with the legs' back-and-forth scissoring. I envisage further elaboration toward mechanisms with more natural geometry, but even these elementary forms can help to explain the structure and dynamics of animals. In particular, Alexander (1988) has identified a wide variety of elastic components in series with animal muscles, and has shown that they store a substantial part of the energy exchanged during a locomotion cycle. Outstanding examples for our purposes are the tendons of the gastrocnemius, plantaris, and deep flexor muscles of the kangaroo, which behave like the stance spring in our model, and the aponeurosis of the longissmus muscle in the backs of dogs and deer, which behaves like the hip spring (in this case producing a scissor oscillation between fore- and hind legs). Our mechanical model suggests that the elastic elements govern the dynamics; they establish the cyclic motion, which the muscles then pump much as a child pumps a swing. A mechanical analogue of this idea is analysed in §8.

Although in practice some pumping is necessary to sustain the running cycle, in principle at least (as in figure 2) passive running can be perfectly conservative. This follows from the symmetry of the gait; if you were shown a film of running as in figure 2, you couldn't tell whether the projector was playing in forward or reverse; one would produce the mirror image of the other. In this respect it faithfully mimics symmetry in animal running, which has been noted by Raibert (1986). Now, if the stance and hip springs are perfectly loss-free, then the only mechanism left for dissipating energy is an impulse on landing (see Appendix 3). However, in a symmetric run, landing is the mirror image of take-off; as there is no impulse at take-off, there is none on landing. Energy would be lost only if asymmetry were introduced, for example by making w in figure 1 non-zero.

4. The mathematics

This section outlines the method for running analysis, while leaving the equations of motion for the Appendix (table 6). Consider a convenient reference point in the stride. We use take-off. At this point the following five state variables can be specified independently.

1. Stance and swing leg angles θ_{C_T}, θ_{F_T}.
2. Angular rates Ω_{C_T}, Ω_{F_T}.
3. Stance extension rate l_{C_T}.

Note that angles are measured from the surface normal, not the vertical (figure 1).

These variables fully determine initial conditions for the flight phase (17), (36), (37). The flight-phase equations are then integrated forward until the leading foot hits the ground. We presume that the foot then stops instantaneously. (On slippery ground a more careful analysis is required, with explicit treatment of sliding (McGeer 1989); however, for surfaces with reasonable friction the zero-slip approximation is almost exact.) If the foot's velocity before landing includes a component normal to the stance axis, then instantaneous stopping requires an impulse; the impulse changes Ω_C, Ω_F, and $\dot{l}_C$ according to (44). Otherwise the stance spring absorbs the impact gradually, and the stance phase begins with the speeds unchanged. In any case the appropriate initial conditions are put into the stance phase equations, and integrated forward until vanishing of the contact force

indicates the next take-off. If the new take-off state is identical to the original, then the cycle is repetitive.

Mathematically one can think in terms of a stride function, $\vec{S}$, mapping take-off conditions from stride k to stride $k+1$:

$$\begin{bmatrix} \theta_{C_T} \\ \theta_{F_T} \\ \Omega_{C_T} \\ \Omega_{F_T} \\ \dot{l}_{C_T} \end{bmatrix}_{k+1} = \vec{S} \begin{pmatrix} \theta_{C_T} \\ \theta_{F_T} \\ \Omega_{C_T} \\ \Omega_{F_T} \\ \dot{l}_{C_T} \end{pmatrix}_k . \tag{1}$$

We want to find an argument that maps onto itself. For any biped that can run passively (some cannot) many such solutions exist. For example, there is nothing especially unique about the cycle in figure 2; a similar motion could proceed over a range of speeds, which implies a range of cycle amplitudes (figure 4). Hence to calculate an individual solution one must specify the amplitude, most conveniently via the take-off stance angle θ_{C_T}. Four state variables then remain to be found. If one knows *a priori* that the cycle must be conservative, then this is the complete search space. However if the cycle is dissipative then the machine must recoup its losses, which can be done most easily by descending a slope. In general the necessary slope (γ) must be found simultaneously with the cyclic state vector.

To describe $\vec{S}$ as merely nonlinear over the search space is to do injustice to its rather unfortunate complexities, so the search cannot be conducted analytically. Instead we resort to Newton's method, whereby an initial estimate for the solution is improved as follows. Define a gradient matrix:

$$\nabla\vec{S} \equiv \left[\frac{\partial\vec{S}}{\partial\theta_{C_T}} \frac{\partial\vec{S}}{\partial\theta_{F_T}} \frac{\partial\vec{S}}{\partial\Omega_{C_T}} \frac{\partial\vec{S}}{\partial\Omega_{F_T}} \frac{\partial\vec{S}}{\partial\dot{l}_{C_T}} \right]. \tag{2}$$

For small changes in the state variables and slope, the change in $\vec{S}$ is approximated by the first-order terms of its Taylor series:

$$\vec{S}\left(\begin{bmatrix} \theta_{C_T} \\ \theta_{F_T} \\ \Omega_{C_T} \\ \Omega_{F_T} \\ \dot{l}_{C_T} \end{bmatrix} \begin{bmatrix} \Delta\theta_{C_T} \\ \Delta\theta_{F_T} \\ \Delta\Omega_{C_T} \\ \Delta\Omega_{F_T} \\ \Delta\dot{l}_{C_T} \end{bmatrix} \right) \approx \vec{S} \begin{pmatrix} \theta_{C_T} \\ \theta_{F_T} \\ \Omega_{C_T} \\ \Omega_{F_T} \\ \dot{l}_{C_T} \end{pmatrix} + \nabla\vec{S} \begin{bmatrix} \Delta\theta_{C_T} \\ \Delta\theta_{F_T} \\ \Delta\Omega_{C_T} \\ \Delta\Omega_{F_T} \\ \Delta\dot{l}_{C_T} \end{bmatrix} + \frac{\partial\vec{S}}{\partial\gamma}\Delta\gamma. \tag{3}$$

Therefore to satisfy the steady-cycle condition, from (1),

$$\begin{bmatrix} \theta_{C_T} \\ \theta_{F_T} \\ \Omega_{C_T} \\ \Omega_{F_T} \\ \dot{l}_{C_T} \end{bmatrix} + \begin{bmatrix} \Delta\theta_{C_T} \\ \Delta\theta_{F_T} \\ \Delta\Omega_{C_T} \\ \Delta\Omega_{F_T} \\ \Delta\dot{l}_{C_T} \end{bmatrix} \approx \vec{S} \begin{pmatrix} \theta_{C_T} \\ \theta_{F_T} \\ \Omega_{C_T} \\ \Omega_{F_T} \\ \dot{l}_{C_T} \end{pmatrix} + \nabla\vec{S} \begin{bmatrix} \Delta\theta_{C_T} \\ \Delta\theta_{F_T} \\ \Delta\Omega_{C_T} \\ \Delta\Omega_{F_T} \\ \Delta\dot{l}_{C_T} \end{bmatrix} + \frac{\partial\vec{S}}{\partial\gamma}\Delta\gamma. \tag{4}$$

As explained earlier we leave θ_{C_T} constant in our solution procedure. Solving for the adjustments required in the remaining take-off variables and the slope leaves:

$$\begin{bmatrix} \Delta\theta_{F_T} \\ \Delta\Omega_{C_T} \\ \Delta\Omega_{F_T} \\ \Delta\dot{l}_{C_T} \\ \Delta\gamma \end{bmatrix} \approx \left(\left[\frac{\partial\vec{S}}{\partial\theta_{F_T}} \frac{\partial\vec{S}}{\partial\Omega_{C_T}} \frac{\partial\vec{S}}{\partial\Omega_{F_T}} \frac{\partial\vec{S}}{\partial\dot{l}_{C_T}} \frac{\partial\vec{S}}{\partial\gamma} \right] - \begin{bmatrix} 00000 \\ 10000 \\ 01000 \\ 00100 \\ 00010 \end{bmatrix} \right)^{-1} \left(\begin{bmatrix} \theta_{C_T} \\ \theta_{F_T} \\ \Omega_{C_T} \\ \Omega_{F_T} \\ \dot{l}_{C_T} \end{bmatrix} - \vec{S} \begin{pmatrix} \theta_{C_T} \\ \theta_{F_T} \\ \Omega_{C_T} \\ \Omega_{F_T} \\ \dot{l}_{C_T} \end{pmatrix} \right). \tag{5}$$

To find a solution, one evaluates (5) iteratively until convergence. If the starting point is reasonable and a solution exists then this technique will find it (to five figures in each state variable) within ten iterations. Note that each iteration involves six evaluations of $\vec{S}$; one with the nominal state vector, and then five more for numerical calculation of the gradients. Each evaluation involves numerical integration of four nonlinear equations (38), (39) through the flight phase, followed by calculation of the speed change on landing (44), followed by numerical integration of three nonlinear equations (50) through the stance phase. Thus one iteration according to (5) calls for intensive computation requiring about 20 s on an IBM AT.

For the initial estimate in Newton's method it is sufficient with most parameter sets to use $\theta_{F_T} = \pi - \theta_{C_T}$, $\Omega_{C_T} = -\Omega_{F_T} = V$, where V is the speed anticipated in the solution, $\dot{l}_{C_T} = 1$ and $\gamma = 0$. Convergence is accelerated by starting from a solution previously obtained for a similar parameter set. Another approach is simply to generate initial conditions at random. This is perhaps naive, but it is also unbiased, and so can reveal behaviour that might otherwise go unnoticed. In fact with this technique we discovered that the cyclic solution is not unique even with θ_{C_T} fixed. Several solutions are listed in the example of table 1. The first of these is just bouncing in place on a steep hill (i.e. $\theta_{C_T} = -\gamma = \theta_{F_T} - \pi$). The next corresponds to normal running. Notice that $\omega_{sc}\tau_0 \approx \pi$ as in figure 2, which indicates that the legs go through half a scissor cycle in one stride. The next two are unusual;

TABLE 1. NEWTON'S METHOD SOLUTIONS FOR PASSIVE RUNNING CYCLES OVER 40 TRIALS WITH RANDOM INITIAL ESTIMATES IN THE RANGE $0 < \theta_{C_T} < \pi/2$; $\pi/2 < \theta_{F_T} < \pi$; $0 < \Omega_{C_T} < 2$; $-2 < \Omega_{F_T} < 0$; $0 < \dot{l}_{C_T} < 2$

(Parameters: $R = 0$; $r_{gyr} = 1/3$; $c = 0.7$; $w = 0$; $K_{leg} = 20$; $K_{hip} = 0.2$; $m_T = 0.8$; $\theta_{C_T} = 0.45$.)

Newton's method converged in 16/40 cases, as follows:

cases	1/40	10/40	4/40	1/40
θ_{F_T}	3.59	2.64	2.30	2.25
Ω_{C_T}	0	1.65	0.98	0.73
Ω_{F_T}	0	−1.22	−0.47	−0.41
$\dot{l}_{C_T}$	arbitrary	0.90	1.28	1.89
γ	−0.45	0	0	0
s	0	1.36	3.03	5.01
τ_b	arbitrary	0.26	1.50	2.81
τ_c	arbitrary	0.48	0.66	0.68
$\omega_{sc}\tau_0$	arbitrary	3.30	9.6	15.6

$\omega_{sc}\tau_0 \approx 3\pi$ and 5π, respectively, so the legs go through 1.5 and 2.5 scissor cycles per stride. That is, the legs cross once or twice during flight, as well as once during stance, and the bounce is more energetic than normal to provide sufficient flight time. Needless to say, here we are interested only in the 'half-scissor' running cycle.

5. Stability

Existence of a repetitive state vector is the essence of passive running. However it is not a sufficient condition; the passive cycle must also be stable with respect to perturbations in the state vector. To investigate stability, suppose that on stride k the take-off conditions are perturbed from the repetitive values by $\Delta\theta_{C_{Tk}}$, $\Delta\theta_{F_{Tk}}$, etc. If the perturbations are small, then the conditions at take-off on stride $k+1$ are accurately estimated by the linear approximation of $\vec{S}$ (3):

$$\begin{bmatrix} \Delta\theta_{C_T} \\ \Delta\theta_{F_T} \\ \Delta\Omega_{C_T} \\ \Delta\Omega_{F_T} \\ \Delta l_{C_T} \end{bmatrix}_{k+1} \approx \nabla\vec{S} \begin{bmatrix} \Delta\theta_{C_T} \\ \Delta\theta_{F_T} \\ \Delta\Omega_{C_T} \\ \Delta\Omega_{F_T} \\ \Delta l_{C_T} \end{bmatrix}_k . \tag{6}$$

This is just a linear difference equation in standard form. Solutions are proportional to z^k, where z is any eigenvalue of $\nabla\vec{S}$. Thus if all eigenvalues have magnitude less than unity, then small disturbances decay over subsequent strides. If not, then disturbances grow and eventually the biped stumbles.

For illustration, return to the example cycle of figure 2. Its eigenvalues and eigenvectors are listed in table 2. There are three modes, which prove to be quite typical of passive running; we will show many more examples. (Similar modes also arise in passive walking (McGeer 1990*a*).)

Table 2. Stride-to-stride stability of the cycle in figure 2

mode	speed	swing		totter	
		mag.	±phase	mag.	±phase
eigenvalue	1	0.22	±1.62	1.65	±2.42
θ_{C_T}	0.13	0.03	±0	0.08	±0
θ_{F_T}	−0.08	0.44	±1.85	0.23	∓2.06
Ω_{C_T}	0.42	0.07	∓2.47	0.13	∓1.07
Ω_{F_T}	−0.72	0.89	∓1.44	0.95	±0.55
l_{C_T}	0.53	0.08	±0.41	0.14	±1.59

The model in this example is conservative, and so on level ground it can run steadily at any speed. Thus if the elements in the take-off state vector are perturbed according to the first eigenvector listed in table 2, then the speed shifts to a new equilibrium. The model is therefore neutrally stable in this 'speed' mode. A dissipative model, however, would have a unique equilibrium speed on any given slope; this would lead to a slowly convergent speed mode, as indicated by figure 5.

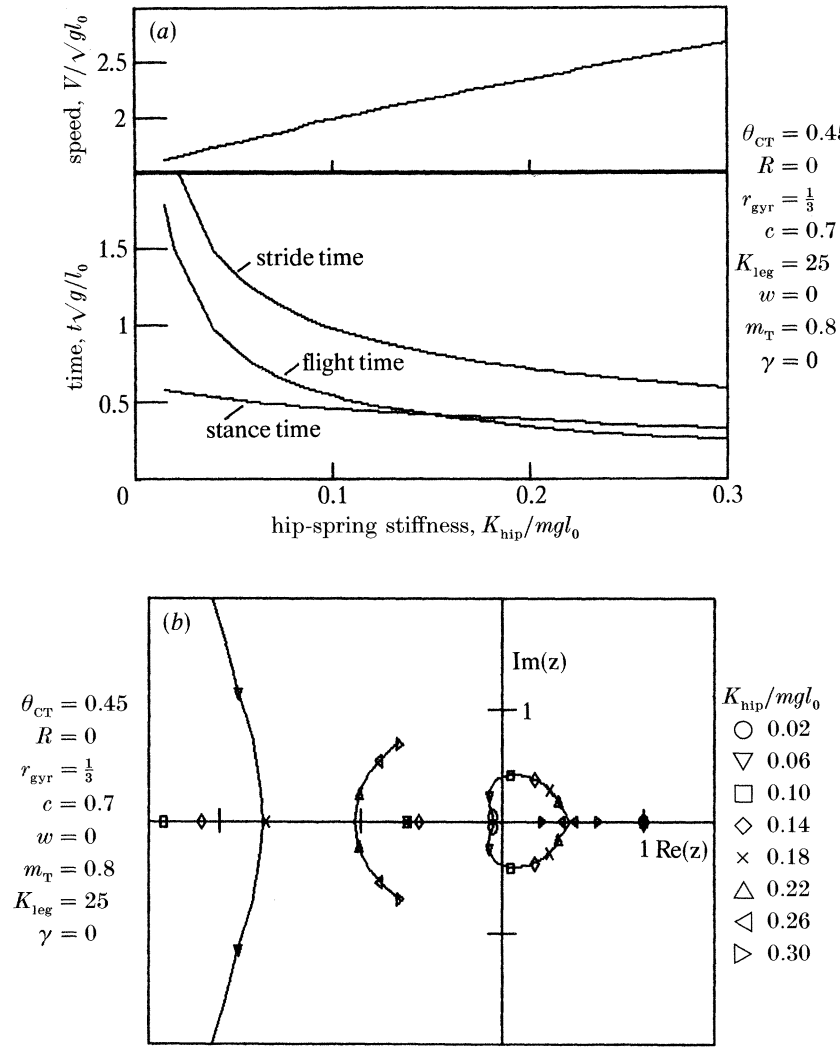

FIGURE 3. The cycle of figure 2 turns out to be unstable. However passive running can be stabilized by making the hip-spring stiffer. (*a*) The resulting decrease in stride period (and a small increase in speed, which is of secondary importance). (*b*) The improvement in stability. Perturbations on the steady cycle scale over k steps in proportion to z^k, where z is one of five stride-to-stride eigenvalues. Here the positions of these eigenvalues are plotted in the form of a locus on the complex plane. With a soft hip spring one conjugate pair of eigenvalues, for the 'totter mode', has magnitude larger than unity; these indicate that the running cycle is unstable. However a sufficiently stiff spring moves these eigenvalues onto the unit circle; running is then neutrally stable with respect to small perturbations.

The next mode is called 'swing' because of the large θ_{F_T} and Ω_{F_T} components. It arises in correcting aberrations in motion of the swing leg, and usually damps quickly.

Finally there is the 'totter' mode, which (at least in walking) is how a passive biped resolves the discrepancy that arises if its initial stride length is inappropriate

to its initial forward speed. The name refers to an oscillation about the steady cycle, which as in this example typically has a period of 2–3 strides. Here the totter mode is unstable.

The totter instability is unacceptable; something must be done. Options are to stabilize by active control, which is discussed in §9, or to change design parameters so that running becomes passively stable. It turns out that although several parameters can be adjusted to some good effect (table 5), only one is especially powerful: cadence. As I have explained, cadence is determined by the scissor frequency, which in turn is most easily adjusted via the stiffness of the hip spring. Thus figure 3 shows the effect of spring stiffness on the stride-to-stride eigenvalues. As K_{hip} increases, the totter eigenvalues tend to diminish until their magnitude reaches unity. Further increase in K_{hip} then changes only the phase of the totter eigenvalues, leaving the magnitude nearly constant. That is, with a sufficiently stiff spring, and hence sufficiently rapid cadence, the totter mode becomes neutrally stable.

Now neutral stability is not quite acceptable, but it turns out that with faster cadence having improved the situation to this point, a little dissipation (which is practically inevitable) then makes the totter mode positively stable (figure 5). By familiar standards the necessary cadence is quite fast. The example of figure 3 calls for $K_{\text{hip}} \geqslant 0.2$, with a corresponding stride period $\tau_0 \leqslant 0.7$ in units of $\sqrt{l_0/g}$. In human terms this implies at least five strides (i.e. 2.5 take-offs by each leg) per second. This rate is at the top end of the human data cited by Margaria (1976), and considerably faster than is indicated by the data of McMahon *et al.* (1987) for jogging.

I should emphasize that these conclusions on stability have been developed for small perturbations from the steady cycle (in the sense of (6)). Naturally this raises the question, how small is small? I will address this question in §10.

6. Speed control

Running is used to achieve high speed, so one might be interested in using the passive running model to explore limiting factors. There are three ways to increase speed. The first method, which was shown in passing by figure 3, is to increase cadence. The limitation is then hip stiffness, but in any case the effect of cadence on speed is relatively weak.

The second method is to increase the stiffness of the stance spring; the result is a shorter contact time and a longer leap through the air. (The data of Margaria (1976) and McMahon *et al.* (1987) indicate that humans rely on an analogue of this method as the primary speed control in running.) The limitation is strength in the stance leg: long-term vertical equilibrium calls for an average force during stance of $mg\tau_0/\tau_c$; the shorter the contact time, the higher the force.

The third method (the only option for a machine with built-in hip and stance stiffnesses) is to increase scissoring amplitude. Figure 4 shows the effect on the running cycle. A key point to note is the minimal effect on cadence; stride period remains close to half the scissor period throughout the speed range. However the fraction of the period in stance decreases with increasing speed, so again leg

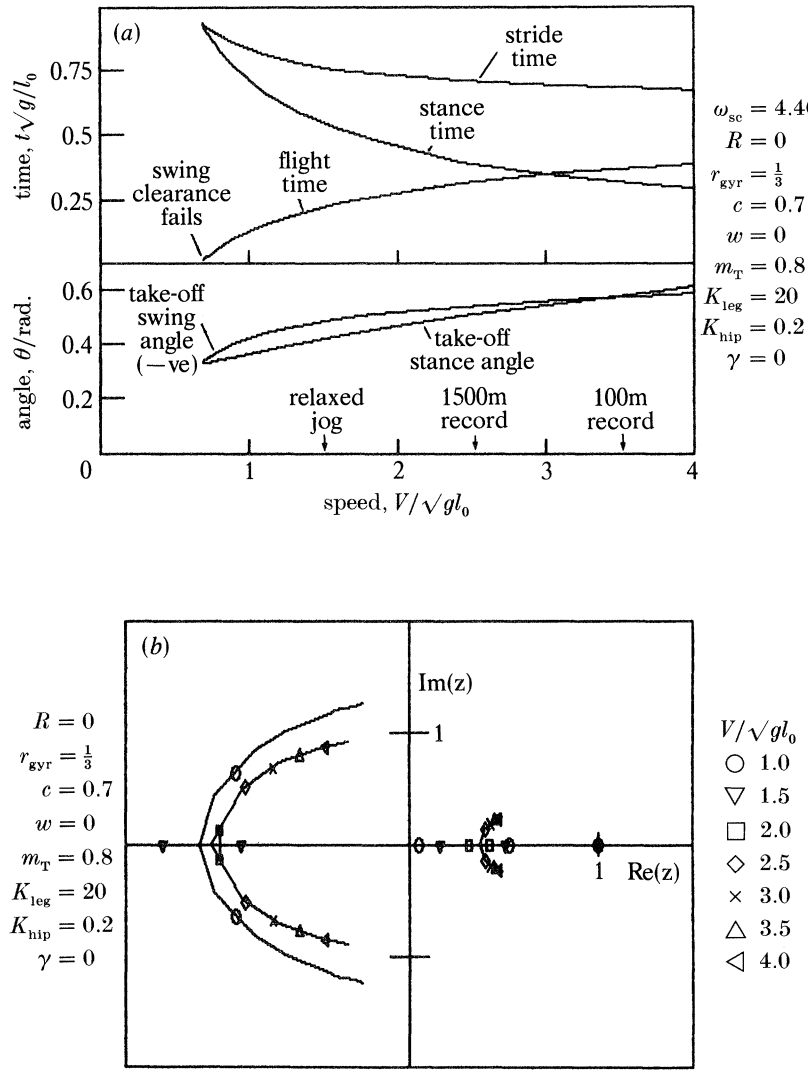

FIGURE 4. Forward speed can be controlled by varying the amplitude of the legs' scissor action. (*a*) Amplitude as a function of speed, and the corresponding variation in cycle timing. Note that although the stance:flight ratio varies with speed, the overall time for one stride remains roughly constant. (*b*) The locus of stride-to-stride eigenvalues against speed. Its features are similar to those of the locus against hip stiffness (figure 3); here, running is unstable at low speed, but stable at high speed.

strength is the limiting factor. Notice that figure 4 also shows a lower limit on speed, which is reached when stance occupies the whole of the cycle, and the flight time goes to zero. This limit is determined by the stance stiffness, and can be shifted (if necessary all the way to zero speed) by making the stance-spring stiffer.

I have included with figure 4 a root locus to show the effect of scissor amplitude on stability. Note especially the totter eigenvalues, which converge along a broad outer arc, split along the negative real axis, merge again, and split onto an inner

arc through the complex plane. This pattern is somewhat canonical: figure 3 showed a similar pattern with hip stiffness as the variable, and one sees much the same pattern varying other parameters as well (for example, stance stiffness, damping, etc.) Therefore the designer can use one parameter to compensate for another. In figure 3, for example, totter stability could be achieved with lower hip stiffnesses if the speed were faster; in figure 4, totter stability could be achieved at lower speed if the hip spring were stiffer.

7. Energy dissipation

Thus far I have confined attention, rather optimistically, to passive running without dissipation. Here we will evaluate dissipative effects, and suggest levels of energy consumption that might be achieved by a practical passive runner. For the present I imagine balancing dissipation by descending a slope, but in the next section, an alternative means of energy supply is analysed.

Downhill running is particularly convenient for evaluating energy consumption, because the slope is equal to specific resistance:

$$SR \equiv \text{resistive force/mass} = \text{mechanical work done/mass} \times \text{distance travelled.} \quad (7)$$

SR is commonly used as a measure of efficiency for all manner of vehicles. In running, contributors to *SR* include joint friction, landing impulses, and aerodynamic drag. I shall evaluate each in turn.

7.1. *Joint friction*

First consider friction in telescoping of the stance leg. Figure 5 shows its effect on gait parameters and *SR*. For convenience in calculations I have taken the friction to be viscous (17), measured by the damping ratio $\zeta = d_{\text{leg}}/\sqrt{4K_{\text{leg}}}$, which one would observe if the model were oscillating vertically on the stance spring. (Some may prefer to measure dissipation by the quality; $Q = 1/2\zeta$. Alternatively one might just note that $\zeta = 0.05$ corresponds to $\approx 50\,\%$ energy loss during each vertical oscillation.) As an example of the damping level that can be achieved in practice, data presented by Raibert *et al.* (1984) indicate that his monopedal hopper had a damping ratio of 0.06 with a pneumatic stance spring. For a passive running machine as in figure 5, this would imply $SR \approx 0.08$ at a speed just below sprinting. Most of this resistance is due to direct frictional dissipation, but there is also a small contribution from a landing impulse (which arises because friction makes the running cycle asymmetric). Substantial improvement could be realized by using a metallic spring rather than a pneumatic cylinder; the cylinder, however, has the advantage of easily adjustable stiffness.

Figure 5 also includes a root locus illustrating the effect of stance damping on stability. As we mentioned earlier, damping stabilizes the totter mode. It also makes the speed mode slowly convergent rather than neutrally stable, as now there is only one steady speed for any given slope.

Next consider friction in the hip joint. This requires careful treatment. The problem is that hip damping makes the foot land with excess forward speed, which tends to trip the machine. Figure 6 shows the consequences. As the damping

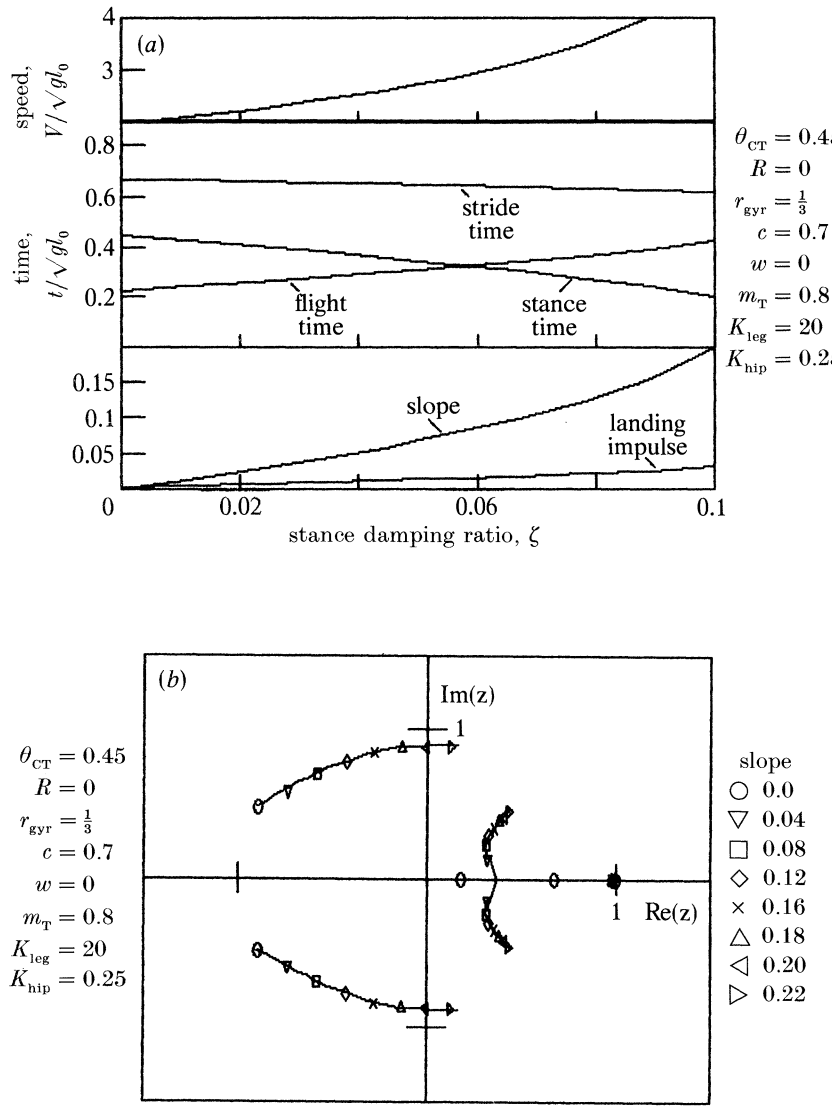

FIGURE 5. Friction in compression of the stance leg drains energy from the passive running cycle, but losses can be made good by running downhill. In this example, the friction is taken to be viscous, and is measured by the damping ratio for vertical oscillations on the stance spring; (*a*) (lower plot) the slope required for steady running, as a function of damping ratio. Most of the energy loss is directly due to friction, but a part is dissipated by an impulse on landing; (*b*) damping moves the stride-to-stride eigenvalues inside the unit circle, and so makes running positively stable.

increases, a negative landing impulse (i.e. a downward pull) is required to stop the foot. (Actually the foot would slip on landing, because a downward impulse is physically impossible; however, the impulsive stop is still a good approximation (McGeer 1989).) Then a bit more damping makes the running cycle disappear completely. Fortunately the cycle can be resuscitated by only a small adjustment

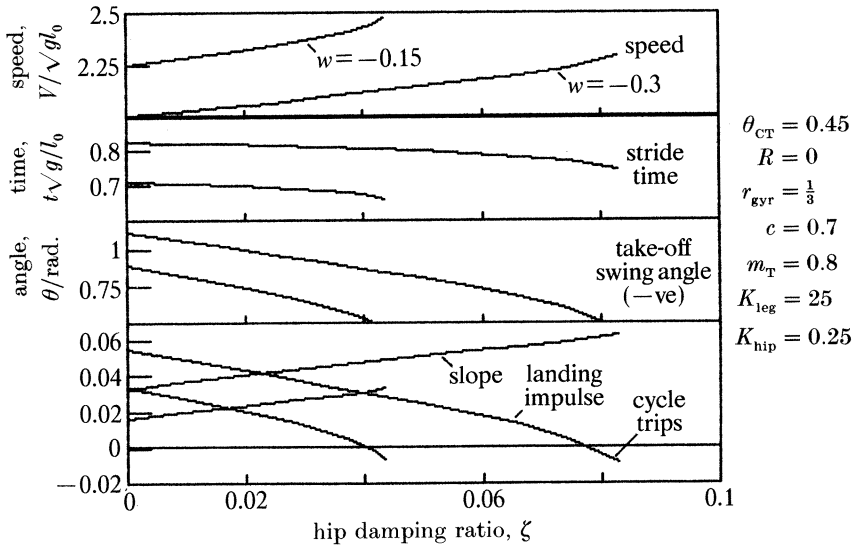

FIGURE 6. Whereas friction in the stance spring can be countered simply by running downhill, friction in the hip requires more careful attention. Hip damping makes the foot land with excess forward speed. Stopping the foot then calls for a negative impulse (i.e. a downward pull), which is not only physically impossible but also dynamically unacceptable. Thus only slight friction at the hip can trip the passive cycle. However the situation is retrieved by shifting each leg's mass centre backward from the leg axis ($w < 0$, see figure 1).

of the leg mass centre. Thus, as shown in the figure, if the mass centre is placed behind the axis of the leg (i.e. $w < 0$) then running can be sustained even with substantial hip friction. (The same is true for walking.) However this adjustment has the unpleasant side effect of destabilizing the totter mode, so active stabilization becomes necessary. Therefore the best strategy is to minimize hip friction in the first instance. We have found ball bearing joints satisfactory for our walking machines, and with similar arrangements we expect that hip friction in a running machine would make only a very minor contribution to *SR*.

7.2. *Unsprung mass*

Landing impulses due to asymmetry, as in figures 5 and 6, make only small contributions to *SR* under any reasonable conditions. However more substantially dissipative impulses arise if the feet have non-zero mass. Energy dissipation can be estimated by imagining a point mass m_f hitting the ground with speed v_{foot_T} and stopping elastically. Then:

$$\Delta E = (1/2)\, m_f\, v_{foot_T}^2. \tag{8}$$

With m_f and v_{foot_T} in dimensionless form, dividing (8) by stride length gives the contribution to *SR*. Also $v_{foot_T} \approx -\dot{l}_{C_T}$ (as landing mirrors take off, and at take-off the foot moves parallel to the leg axis). Therefore:

$$(\Delta E/mgs) \approx m_f(\dot{l}_{C_T}^2/2s). \tag{9}$$

Even in a sprint $\dot{l}_{C_T}^2/2s < 1$, so at most this contribution is numerically equal to m_f. At slower speed it is only half that or less. For a carefully designed machine m_f can be quite small; Raibert (1986) achieved $m_f \approx 0.01$ in his quadruped runner, even with each foot incorporating part of a pneumatic actuator. That leaves unsprung mass a very minor contributor to the total *SR*.

Unfortunately the figures are not so good for a human runner. Although telescoping legs cannot transmit lengthwise impulses, knee joints can; consequently, humans have an effectively higher unsprung mass. Force measurements by McMahon *et al.* (1987) indicate a vertical impulse of ≈ 0.08 (normalized by $m\sqrt{gl_0}$) in jogging. An impulse of this magnitude from a machine with telescoping legs would involve $m_f \approx 0.1$! Of course for nature telescoping legs are not an option. (One wonders what course evolution might have taken had the choices been otherwise!)

7.3. *Aerodynamic drag*

Usually one estimates aerodynamic force by using the formula:

$$F_D = \tfrac{1}{2}\rho V^2 A_f C_D. \tag{10}$$

Normalizing by m, g, and l_0 gives the contribution to specific resistance:

$$\frac{F_D}{mg} = \frac{1}{2}\frac{V^2}{gl_0}\frac{\rho A_f l_0}{m} C_D. \tag{11}$$

The first RHS quotient is just the square of the normalized speed. The second quotient is the normalized mass of the box of air roughly enclosing the model. On Earth this number is of the order 0.01. Finally Hoerner (1965) suggests $C_D \approx 1$ for a human. The aerodynamic contribution to *SR* then amounts to about 0.01 in a jog, and 0.05 in a sprint ($V = 3.5$). These figures are similar to estimates made by Margaria (1976) from experimental data. Considerable improvement could be realized by streamlining, and so reducing C_D.

7.4. *Total specific resistance*

Table 4 lists conservative estimates for the various contributions to the specific resistance of running, and the corresponding power requirements. These confirm that, as the jogger already knows, running is hard work. For example, scaling the

TABLE 3. AN ESTIMATE OF SPECIFIC RESISTANCE IN RUNNING

mechanism	parameter	resistance			means for improvement
		jogging	running	sprinting	
stance damping	d_{leg}	0.05	0.07	0.10	efficient leg spring, bearings
hip damping	d_{hip}	<0.005	0.01	0.01	efficient hip spring, bearings
normal impulse	asymmetry	<0.005	<0.005	<0.005	symmetry
unsprung mass	m_f	<0.005	<0.005	0.01	structural design
aerodynamic drag	C_D	0.01	0.03	0.06	streamlining
total	*SR*	0.06	0.11	0.18	cf. ≈ 0.02 in walking
power	$SR \times V$	0.09	0.28	0.63	normalized by $mg\sqrt{gl_0}$

power to suit a human-sized machine gives a figure of 0.3 h.p.† for jogging, and 2 h.p. for sprinting. These figures are comparable to those for humans. Margaria (1976) shows measurements of oxygen uptake while running on a treadmill (and hence free of aerodynamic drag) that indicate energy consumption corresponding to $SR \approx 0.43$, independent of speed in the range $0.8 < V < 1.9$ (fast jogging and below). To find the mechanical work this figure must be multiplied by the conversion efficiency of muscle; a value of 0.25 is considered representative, so SR comes out to be about 0.11.

Incidentally a jogger also knows that walking is more economical than running, and the passive walking model (McGeer 1990*a*) bears out this experience. The SR in walking at $V \approx 0.25$ is about 0.02, and the mechanical power is only about 0.015 h.p.

8. Energy supply

Consider means for overcoming the specific resistance. I consider two alternatives to running downhill: torqueing about the hip, and thrusting with the stance leg.

8.1. *Stance torque*

Suppose that during contact a torque T_T is applied to the stance leg, in addition to the torques caused by the hip spring and gravity. This new component does additional work on the leg, and so adds energy to the cycle amounting in symmetric running to $2T_T\theta_{C_T}$. Then the energy balance for steady running on slope γ is:

$$2T_T\theta_{C_T} \approx s(\gamma_g - \gamma), \tag{12}$$

where γ_g is the slope for running under gravity power. Hence the required torque is:

$$T_T \approx \frac{s}{2\theta_{C_T}}(\gamma_g - \gamma). \tag{13}$$

Torque application according to this strategy turns out to harmonize well with the passive running cycle, with little effect on gait or stability. The only problem is that the torque has to be produced by pushing against something. The swing leg cannot serve as the reaction partner; its inertia is too small, and in any case it should be left free to avoid problems similar to those produced by hip damping. A better alternative is to push against a leaning torso. Thus if a torso with centroid some distance c_T from the hip is held at angle θ_T by reacting against the stance leg, then the torque produced is:

$$T_T = m_T c_T \sin(\theta_T + \gamma). \tag{14}$$

The torso angle required for running on slope γ therefore satisfies, from (13),

$$\sin(\theta_T + \gamma) \approx s/(2m_T c_T \theta_{C_T})(\gamma_g - \gamma). \tag{15}$$

For illustration, take $c_T = 0.3$. Then with gait parameters as in the example of table 1, $d\theta_T/d\gamma$ works out to be approximately equal to 6. Presumably one would be prepared to lean the torso by as much as 0.5 radian or so; this would be sufficient for steady jogging on slopes within $\approx \pm 0.1$ radian of γ_g. Thus hip torque offers a useful but somewhat limited range of capability. For greater range one would use stance thrusting.

† 1 h.p. = 745.7 J s^{-1}.

8.2. *Stance thrust*

Stance thrusting can be done in any number of ways. One simple option is negative damping, i.e. with an incremental force proportional to $\dot{l}_C$. This is unattractive, however, because just as positive damping improves the stability of the totter mode (figure 5), so negative damping degrades stability. A more promising option turns out to be 'ramping' the relaxed position of the stance spring, according to:

$$l_{zf} = l_0 + l_\theta \theta_C. \tag{16}$$

Thus, in general, the stance force is:

$$F_{leg} = K_{leg}(l_{zf} - l_C) - d_{leg}\dot{l}_C. \tag{17}$$

Figure 7 shows the value of l_θ required for steady running with various scissor amplitudes, as a function of slope. The cycle remains stable right across the range of possibilities shown in the figure; thus running can be sustained at any desired speed and slope by appropriate choice of l_θ. However it turns out that l_θ causes the same tripping problem as arises with hip friction; to avoid the problem, as figure 7 indicates, vigorous thrusting must be accompanied by backward shifting of leg mass. Actually humans may use the same technique. When running on the level we let support roll all the way from heel to toe, but when climbing we run only on our toes. This shifts each leg's mass centre backward with respect to an axis connecting support point and hip.

We have now described three different media for supplying energy to the running cycle: a downhill slope, hip torque, and stance thrust. All are effective

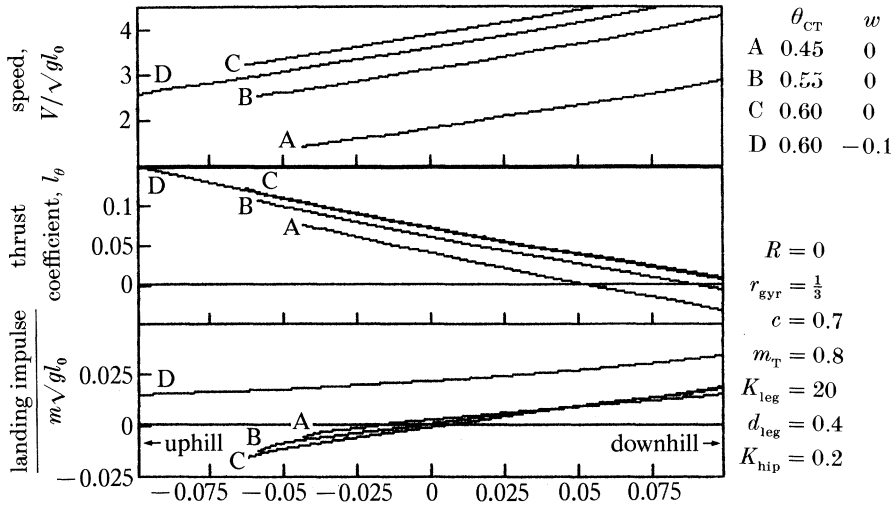

FIGURE 7. As an alternative to running downhill, energy can be supplied by thrusting with the stance leg. In this example the thrust is generated by 'ramping' the equilibrium length of the spring, according to $l_{zf} = l_0 + l_\theta \theta_C$. Some care is required when using this technique, because sufficiently large l_θ makes the landing impulse negative and so 'trips' the running cycle. To compensate for this effect, the legs' mass centres must be offset backwards. A steeper climb requires more l_θ, and so more offset. When climbing, humans introduce a similar offset by running on the balls of the feet.

because a passive biped, like any oscillator, naturally channels incoming energy into its preferred mode of motion.

9. Active stabilization

Although passive running can be made stable by using a sufficiently fast cadence, recovery from disturbances is still rather slow, and moreover provision for fast cadence may be mechanically inconvenient. Consequently active stabilization is desirable, and modulation of the energy supply, particularly by stance thrusting, is suitable for the purpose. To choose an appropriate control strategy we return to the linearized stride-to-stride equations (6). For control one includes the gradient with respect to l_θ. Then the equations become:

$$\begin{bmatrix} \Delta\theta_{C_T} \\ \Delta\theta_{F_T} \\ \Delta\Omega_{C_T} \\ \Delta\Omega_{F_T} \\ \Delta\dot{l}_{C_T} \end{bmatrix}_{k+1} \approx \nabla\vec{S} \begin{bmatrix} \Delta\theta_{C_T} \\ \Delta\theta_{F_T} \\ \Delta\Omega_{C_T} \\ \Delta\Omega_{F_T} \\ \Delta\dot{l}_{C_T} \end{bmatrix}_k + \frac{\partial\vec{S}}{\partial l_\theta}\Delta l_{\theta k}. \tag{18}$$

As an example take the cycle of figure 2, which has an unstable totter mode (table 2). Its gradient matrices are as follows:

$$\nabla\vec{S} = \begin{bmatrix} -1.36 & 0.002 & 0.01 & 0.013 & 0.59 \\ -1.26 & 1.39 & 0.52 & 0.70 & 0.91 \\ -1.73 & 0.47 & 0.26 & 0.27 & 1.46 \\ -6.34 & -3.37 & -2.92 & -1.49 & -0.06 \\ 0.51 & -0.67 & 0.70 & -0.38 & -0.30 \end{bmatrix}, \tag{19}$$

$$\frac{\partial\vec{S}}{\partial l_\theta} = \begin{bmatrix} 1.88 \\ 1.16 \\ -0.41 \\ 6.27 \\ 3.60 \end{bmatrix}. \tag{20}$$

To choose a control law, we apply the well-known linear-quadratic algorithm (see, for example, Bryson & Ho (1975)). With equal weights on the control and state variables, it specifies feedback gains as follows:

$$\Delta l_\theta = [-0.012\ 0.292\ -0.027\ 0.147\ 0.228] \begin{bmatrix} \Delta\theta_{C_T} \\ \Delta\theta_{F_T} \\ \Delta\Omega_{C_T} \\ \Delta\Omega_{F_T} \\ \Delta\dot{l}_{C_T} \end{bmatrix}. \tag{21}$$

Notice that to implement this control law one need measure the state variables only at take-off. The motion during the rest of the stride is treated as a black box

whose internal operations one can simply ignore. This makes for simple implementation, and satisfactorily stable stride-to-stride modes as listed in table 3. Moreover this technique can be used not only to stabilize steady running, but also to vary footfalls from one stride to the next (cf. McGeer (1988) for walking).

TABLE 4. ACTIVE STABILIZATION OF THE CYCLE OF FIGURE 2

mode	1	2	3	4, 5	
				mag.	±phase
eigenvalue	−0.004	−0.52	0.70	0.22	±0.44
θ_{C_T}	0.06	0.03	0.05	0.19	±0
θ_{F_T}	−0.43	−0.33	0.74	0.48	±1.15
Ω_{C_T}	−0.05	0.06	−0.59	0.34	∓2.99
Ω_{F_T}	0.90	0.94	−0.06	0.74	∓1.93
$\dot{l}_{C_T}$	0.06	−0.07	−0.31	0.26	∓0.10

10. LARGE PERTURBATIONS

Our small-perturbation stability analyses indicate the rate of recovery from a disturbance, but they do not address the practical question of how much disturbance the running cycle can tolerate. To investigate the latter question one must numerically integrate the exact stride-to-stride function (1) over a series of strides. A few examples will indicate the possibilities.

Consider first a passive cycle made inherently stable by stance damping. Figure 8 shows transients following perturbations in proportion to its totter-mode eigenvector. In the first example the perturbation is sufficiently small that the transient is fit reasonably well by the linearized stride-to-stride equations (6). However in the second the perturbation is doubled, and the transient departs markedly from the linear fit. Moreover the first example shows a gradual convergence, corresponding to the 'slow' totter eigenvalues; however, the second example shows a gradual divergence, which leads eventually to toppling. Larger initial perturbations, in either the positive or negative sense, topple the machine more quickly.

Now consider perturbation of an actively stabilized running cycle, as discussed in §9. Figure 9 shows the transient following a perturbation in the most lightly damped mode from table 3. If the small-perturbation analysis held then the transient would show a monotonic convergence at $z = 0.70$; it doesn't, however, so the initial perturbation is not 'small'. The perturbation is right at the toppling limit, which is more sharply defined than in the preceding example. Excursions within the limit are rapidly corrected by the active controller; excursions outside the limit cause toppling after only a few strides.

11. FOOT RADIUS

A further variation on the model of figure 1 deserves some attention: foot radius, which affects the motion by moderating centrifugal effect. Figure 10 illustrates the effects of varying foot radius on gait parameters and stability. Also shown is a result based on approximating the rebound during stance. The approximation is somewhat comparable to that of McMahon *et al.* (1987), but includes centrifugal

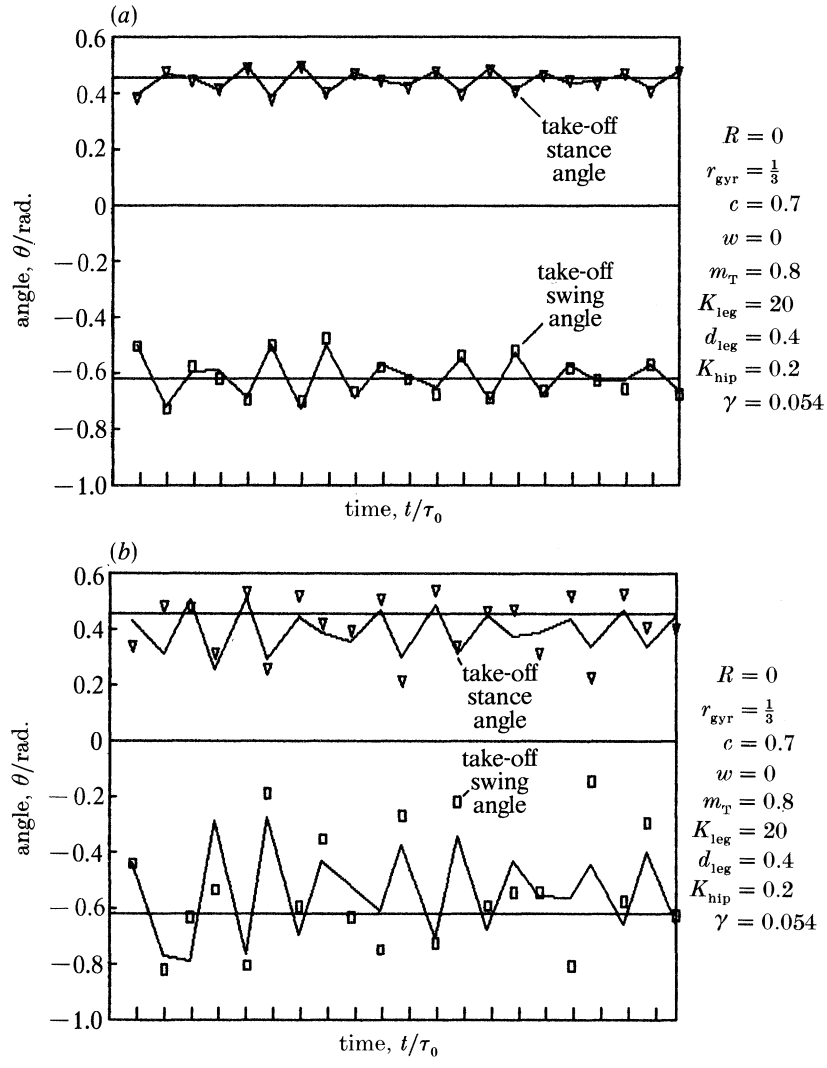

FIGURE 8. This example shows the transient following an initial excitation of the totter mode of an inherently stable machine. Its totter eigenvalues are $z = 0.96e^{\pm 2.7i}$. Hence the transient involves a slow oscillatory decay. Symbols show the stance and swing angles at take-off, as calculated using the exact stride function. Lines show the best fit by the linearized stride-to-stride equations. In (*a*) the initial excitation is small, so the subsequent transient is well fit by the linearized equations. However, in (*b*) the excitation is almost large enough to make the machine stumble, and the linear fit is poor.

terms. Linearize the leg-compression equation (50) with respect to legs-vertical, and take $\Omega_F = -\Omega_C$ to be constant; the equation then becomes:

$$\ddot{l}_C + \omega_l'^2 \Delta l_C = \omega_l' \Delta l_{eq}, \tag{22}$$

where:
$$\omega_l'^2 \equiv K_{leg} - \Omega_C^2, \tag{23}$$

and,
$$\Delta l_{eq} \equiv 1/\omega_l'^2([l_0 - R - (1 - m_T)(l_0 - c)]\Omega_C^2 - 1). \tag{24}$$

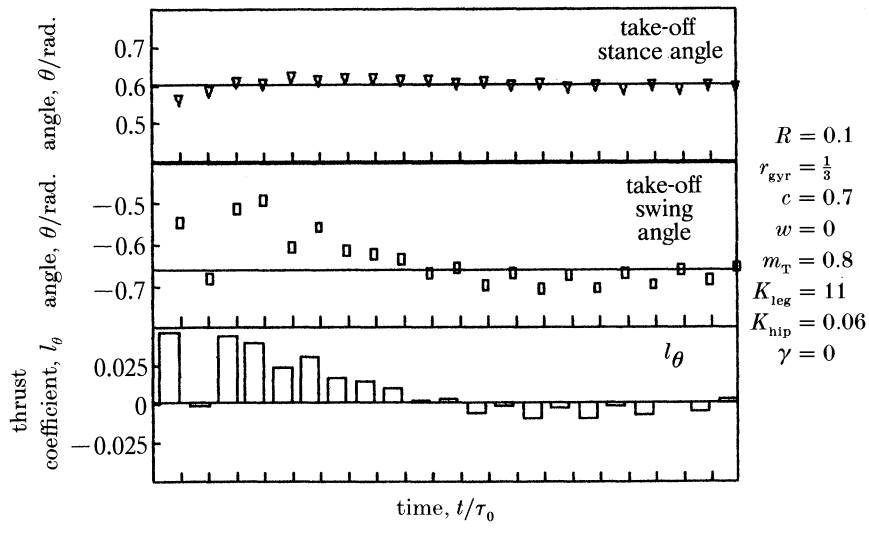

FIGURE 9. Here the transient follows a perturbation on the cycle of figure 2. The amplitude of the perturbation is just below the stumbling limit. This cycle is passively unstable, so we stabilize actively via stride-to-stride adjustment of stance thrust (l_θ).

If $\Omega_C = 0$ then this is just the equation for vertical oscillation on the stance spring. The equilibrium in this case is $\Delta l_{eq} = -1/\omega_l^2$, or $-mg/K_{leg}$ in dimensional terms. But if Ω_C is non-zero, then centrifugal effect both 'softens' the spring and shifts the equilibrium upward. In running centrifugal effect is normally more powerful than gravity, so the spring would actually be stretched in equilibrium. R affects the equilibrium position, and hence the stance time, as follows: solving (22) for the bouncing motion, with initial conditions $\Delta l_C = 0$, $\dot{l}_C = -\dot{l}_{C_T}$ gives:

$$\Delta l_C = \Delta l_{eq}(1 - \cos \omega_l' \tau) - (\dot{l}_{C_T}/\omega_l') \sin \omega_l' \tau. \tag{25}$$

Stance ends when next $\Delta l_C = 0$; thus τ_c satisfies:

$$(1 - \cos \omega_l' \tau_c)/\sin \omega_l' \tau_c = (-\dot{l}_{C_T}/\omega_l' \Delta l_{eq}) \equiv -v_O. \tag{26}$$

Solving for τ_c gives:

$$\tau_c = (1/\omega_l') \arcsin (2v_O/1 + v_O^2). \tag{27}$$

Normally $\pi/2 < \omega_l' \tau_c < \pi$.

Evaluating (27) by using $\dot{l}_{C_T}$ and Ω_C from the exact cycle calculation produces the 'stance approximation' in figure 10. The approximation certainly isn't perfect, but it is close enough to demonstrate that centrifugal effect is the mechanism whereby foot radius influences the running cycle. The direct result is an increase in τ_c with foot radius. This in turn has repercussions. First, if θ_{C_T} is fixed then increasing τ_c implies decreasing speed, and decreasing speed implies reduced stability (cf. figure 4). Furthermore, as $\tau_0 = \tau_c + \tau_b$ is essentially fixed by the scissor period, an increase in τ_c causes a decrease in τ_b. When τ_b becomes too small the cycle vanishes, so in the example of figure 10 passive running cannot be sustained

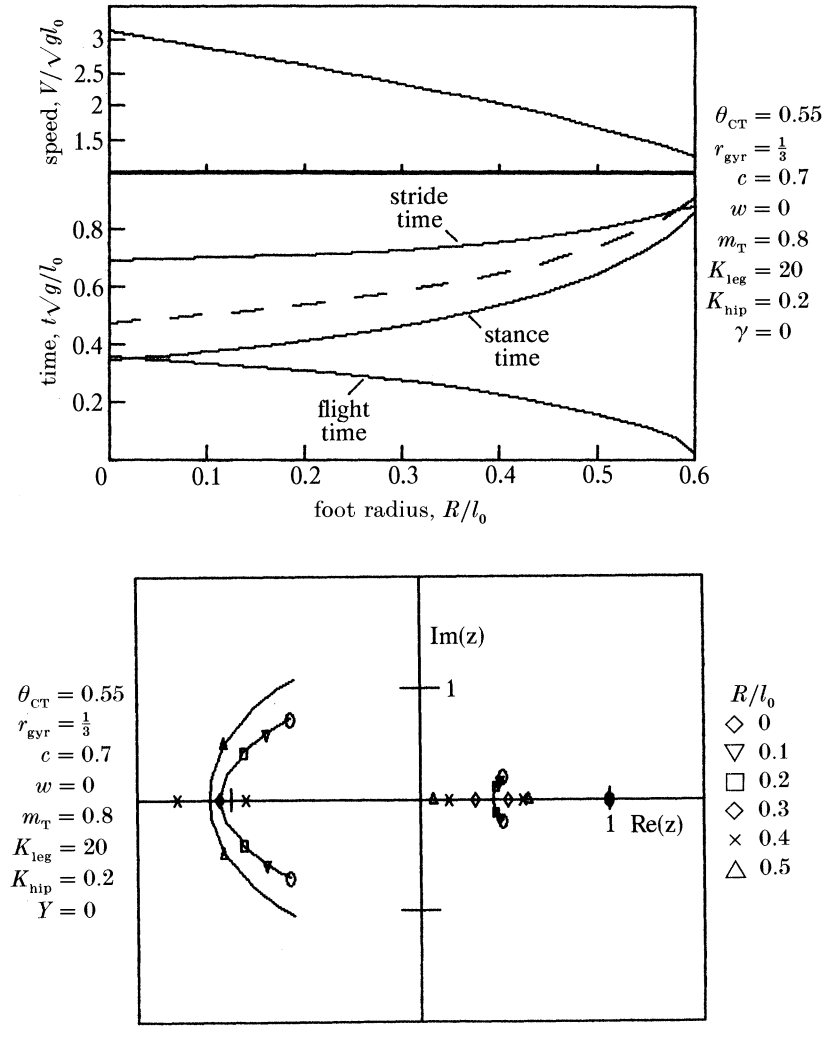

FIGURE 10. (*a*) shows the cycle timing and forward speed of bipeds having various foot radii, and common values for all other parameters, including θ_{C_T}. The direct result of increasing R is reduction in centrifugal effect. The dashed curve shows a consequent increase in τ_c predicted by an approximate one-dimensional model for the stance rebound; this is verified by exact cycle calculations. Increasing stance time implies decreasing flight time and speed; at some point the flight phase becomes untenably short, and the cycle vanishes. (*b*) A corresponding destabilization of the totter mode. The instability can be attributed to the decrease in speed (cf. figure 4), which could be recovered by increasing θ_{C_T} or K_{leg}.

with big feet. (However bigger feet can be accommodated by a compensatory change in another parameter, for example increasing K_{leg}.)

We expect that these effects are not limited to semicircular feet; other shapes should produce similar results. The key factor is translation of the support point during stance. In symmetric running this is:

$$\Delta y = 2\theta_{C_T} R. \tag{28}$$

For example in human running one might take Δy to be the distance from the heel to the ball of the foot. This is about 1/4 of the leg length, so with $\theta_{C_T} = 0.6$ as in figure 2, the equivalent R comes out to 0.2. Of course the differences between this model and a human, in legs as well as feet, make this estimate rather rough. The human jogging gait measured by McMahon *et al.* (1987) was best matched by a passive model with $R = 0.1$ (figure 2).

12. Conclusion

Table 5 lists the parameters in our running model, and summarizes the effects of parameter variations on gait. These provide for a considerable range of behaviour, all based upon the passive bounce-and-scissor oscillation. Moreover, Thompson & Raibert (1989) have shown with their monopedal model that an entirely different mechanism can run by using the same dynamics. The question of obvious interest for human locomotion is, what about a more anthropomorphic model? I suspect that the most important modifications in this direction, ordered by priority, are as follows: (i) knees with torsional springs to replace the telescoping legs; (ii) plantar-flexing feet, again with springs (see Ker *et al.* (1987) for evidence of such springs in human feet); (iii) a torso; (iv) three-dimensionality, particularly swinging of the hips.

As I mentioned earlier, studies of walking indicate that modifications of this sort can be made without substantially disrupting the dynamics of the original model. Miura & Shimoyama (1984) provide further demonstration of this point, particularly with respect to decoupling of fore/aft and side-to-side motions. Hence

Table 5. Major effects of parameter variations on the running cycle

(Signs indicate the effect of a positive parameter increment; ( ), applies only for cycles with dissipation.)

parameter	τ_b	τ_c	τ_0	V	γ	stability	impulse	figure	comments
θ_{C_T}	+	−	0	+	(+)	+	(+)	4	effective for speed control
R	−	+	0	−	(−)	−	(−)	10	foot model
r_{gyr}	0	0	0	0	0	+	(+)	(McGeer 1989)	with K_{hip} adjusted for constant ω_{sc}
c	0	0	0	0	(+)	+	(−)	(McGeer 1989)	with K_{hip} adjusted for constant ω_{sc}
w	−	−	−	+	±	+	−	6	compensates for d_{hip}, l_0
m_T	0	−	−	+	(+)	+	(−)	(McGeer 1989)	with K_{hip} adjusted for constant ω_{sc}
K_{leg}	+	−	0	+	0	+	(−)	(McGeer 1989)	effective for speed control
d_{leg}	+	−	0	+	+	+	+	5	main dissipation mechanism
K_{hip}	−	−	−	+	0	+	0	3	key stability parameter through ω_{sc}
d_{hip}	0	0	0	0	+	+	−	6	must be compensated by w
l_0	−	+	0	−	−	−	−	7	energy supply, active stabilization
T_T	0	0	0	0	−	+	−	(McGeer 1989)	energy supply through torso leaning

I am optimistic that more anthropomorphic models will prove capable of passive running. With that established, the next question would be whether tendons and other elastic structures have the stiffness and damping properties called for by the mechanical model, and whether muscle action can thus be limited to pumping and modulation of a fundamentally passive cycle. Such a line of study, if successful, would ultimately allow accurate quantitative treatment of running physiology from the governing dynamical principles, and perhaps suggest methods for improving performance.

But whatever its success in explaining natural locomotion, the passive running idea is certainly applicable to design of robots. Such machines are under development, particularly by Raibert (1986), with a view towards locomotion over terrain that is not accessible to wheeled vehicles. Legged machines designed to run (or walk) passively promise mechanical simplicity, relative ease of control, and lower specific resistance than alternative candidates, namely tank-like vehicles or devices with large, soft wheels. The bounce-and-scissor oscillation would serve as their foundation for mobility, to be pumped and modulated for adaptation to rough terrain, e.g. to land on randomly spaced footholds, or to jump over obstacles. Of course, to do this successfully, a robot would first have to be sufficiently perceptive to recognize footholds and obstacles; unfortunately the perception problem is much more difficult than the dynamics and control!

Appendix 1. Summary of dynamics equations

Tables 6 and 7 summarize the equations necessary for evaluating the stride function (1). McGeer (1989) gives the derivations in full.

Table 6. Equations required for evaluation of the stride function

phase	flight	stance
translational	(38)	(50)
rotational	(39)	(50)
constitutive	(40)	(17), (40), (16), (13)
geometric	(30), (31), (32)	(30), (31), (32), (33)

Table 7. Events triggering a switch between boundary conditions

flight → stance	$l_C - l_{zf} = 0$ (43), (16) (foot strike)
stance → flight	$F_{leg} = 0$ (17) (force vanishing)

Appendix 2. Flight phase

Define:

$$\hat{x}_C = \begin{bmatrix} \cos\theta_C \\ \sin\theta_C \end{bmatrix}. \tag{29}$$

$$\vec{g} = \begin{bmatrix} -\cos\gamma \\ \sin\gamma \end{bmatrix}, \tag{30}$$

$$\vec{r}_{HC} = (l_0 - c)\begin{bmatrix} -\cos\theta_C \\ -\sin\theta_C \end{bmatrix} + w\begin{bmatrix} -\sin\theta_C \\ \cos\theta_C \end{bmatrix}, \tag{31}$$

$$\vec{r}_{\mathrm{HF}} = (l_0 - c)\begin{bmatrix}\cos\theta_{\mathrm{F}}\\ \sin\theta_{\mathrm{F}}\end{bmatrix} + w\begin{bmatrix}\sin\theta_{\mathrm{F}}\\ -\cos\theta_{\mathrm{F}}\end{bmatrix}, \tag{32}$$

$$\vec{r}_{\mathrm{PH}} = \begin{bmatrix}R\\ 0\end{bmatrix} + (l_{\mathrm{C}} - R)\begin{bmatrix}\cos\theta_{\mathrm{C}}\\ \sin\theta_{\mathrm{C}}\end{bmatrix}, \tag{33}$$

$$I_{\mathrm{H}} \equiv m_{\mathrm{leg}}(r_{\mathrm{gyr}}^2 + (1 - m_{\mathrm{leg}})|\vec{r}_{\mathrm{HC}}|^2), \tag{34}$$

$$I_X \equiv -m_{\mathrm{leg}}^2\, \vec{r}_{\mathrm{HC}} \cdot \vec{r}_{\mathrm{HF}}. \tag{35}$$

Then the position and velocity of the overall mass centre at the start of the flight phase are:

$$\begin{aligned}\vec{r}_{O/\mathrm{CM}} &= \hat{y}R\theta_{\mathrm{C}} + \vec{r}_{\mathrm{PH}} + \vec{r}_{H/\mathrm{CM}}\\ &= \hat{y}R\theta_{\mathrm{C}} + \vec{r}_{\mathrm{PH}} + m_{\mathrm{leg}}(\vec{r}_{\mathrm{HC}} + \vec{r}_{\mathrm{HF}}),\end{aligned} \tag{36}$$

$$\begin{aligned}\vec{V}_{\mathrm{CM}} &= \frac{d\vec{r}_{O/\mathrm{CM}}}{dt}\\ &= \hat{x}_{\mathrm{C}}\dot{l}_{\mathrm{C}} + \hat{y}R\Omega_{\mathrm{C}} - (\vec{r}_{\mathrm{PH}} - R\hat{x} + m_{\mathrm{leg}}\vec{r}_{\mathrm{HC}}) \times \Omega_{\mathrm{C}} - m_{\mathrm{leg}}\vec{r}_{\mathrm{HF}} \times \Omega_{\mathrm{F}}\\ &= \hat{x}_{\mathrm{C}}\dot{l}_{\mathrm{C}} - (\vec{r}_{\mathrm{PH}} + m_{\mathrm{leg}}\vec{r}_{\mathrm{HC}}) \times \Omega_{\mathrm{C}} - m_{\mathrm{leg}}\vec{r}_{\mathrm{HF}} \times \Omega_{\mathrm{F}}.\end{aligned} \tag{37}$$

The equations of motion are:

$$\vec{V}_{\mathrm{CM}} = \vec{g}, \tag{38}$$

$$\begin{bmatrix}I_H & I_X\\ I_X & I_H\end{bmatrix}\begin{bmatrix}\dot{\Omega}_{\mathrm{C}}\\ \dot{\Omega}_{\mathrm{F}}\end{bmatrix} + \begin{bmatrix}0 & m_{\mathrm{leg}}^2\vec{r}_{\mathrm{HC}} \times \vec{r}_{\mathrm{HF}}\\ m_{\mathrm{leg}}^2\vec{r}_{\mathrm{HF}} \times \vec{r}_{\mathrm{HC}} & 0\end{bmatrix}\begin{bmatrix}\Omega_{\mathrm{C}}^2\\ \Omega_{\mathrm{F}}^2\end{bmatrix} = \begin{bmatrix}T_{\mathrm{hip}}\\ -T_{\mathrm{hip}}\end{bmatrix}. \tag{39}$$

Usually T_{hip} is chosen according to:

$$T_{\mathrm{hip}} = K_{\mathrm{hip}}(\theta_{\mathrm{F}} - \pi - \theta_C) + d_{\mathrm{hip}}(\Omega_{\mathrm{F}} - \Omega_{\mathrm{C}}). \tag{40}$$

I have mentioned that the cadence is set by the scissor frequency, and this can be calculated by linearizing the rotational equations (39) for small perturbations from legs-parallel. The result is that:

$$\omega_{\mathrm{sc}} = \sqrt{(2K_{\mathrm{hip}})/(m_{\mathrm{leg}}(r_{\mathrm{gyr}}^2 + |\vec{r}_{\mathrm{HC}}|^2))}, \tag{41}$$

and:

$$\zeta_{\mathrm{sc}} = (\omega_{\mathrm{sc}}\, d_{\mathrm{hip}})/(2K_{\mathrm{hip}}). \tag{42}$$

Appendix 3. Impulsive landing

Landing occurs when the foot touches the ground; mathematically the condition is that:

$$l_{zf} = \frac{x_{\mathrm{CM}} - R - m_{\mathrm{leg}}(\vec{r}_{\mathrm{HC}} + \vec{r}_{\mathrm{HF}}) \cdot \hat{x}}{\cos\theta_{\mathrm{C}}} + R. \tag{43}$$

Then post-landing speeds then satisfy:

$$\begin{bmatrix} I_C & I_{FC} & I_{LC} \\ I_{FC} & I_F & I_{LF} \\ I_{LC} & I_{LF} & 1 \end{bmatrix} \begin{bmatrix} \Omega_C^+ \\ \Omega_F^+ \\ \dot{l}_C^+ \end{bmatrix} = \begin{bmatrix} I_H & I_X \\ I_X & I_H \\ 0 & 0 \end{bmatrix} \begin{bmatrix} \Omega_C^- \\ \Omega_F^- \end{bmatrix} + \begin{bmatrix} (\vec{r}_{PH} + m_{leg}\vec{r}_{HC}) \times \vec{V}_{CM}^- \\ m_{leg}\vec{r}_{HF} \times \vec{V}_{CM}^- \\ \hat{x}_C \cdot \vec{V}_{CM}^- \end{bmatrix}. \tag{44}$$

Appendix 4. Stance phase

Define:

$$I_C \equiv m_{leg}(r_{gyr}^2 + |\vec{r}_{PH} + \vec{r}_{HC}|^2) + (1 - m_{leg})|\vec{r}_{PH}|^2, \tag{45}$$

$$I_F \equiv m_{leg}(r_{gyr}^2 + |\vec{r}_{HF}|^2), \tag{46}$$

$$I_{FC} \equiv m_{leg}\vec{r}_{HF} \cdot \vec{r}_{PH}, \tag{47}$$

$$I_{LC} \equiv -(\vec{r}_{PH} + m_{leg}\vec{r}_{HC}) \cdot \hat{y}_C, \tag{48}$$

$$I_{LF} \equiv -m_{leg}\vec{r}_{HF} \cdot \hat{y}_C. \tag{49}$$

Then:

$$\begin{bmatrix} I_C & I_{FC} & I_{LC} \\ I_{FC} & I_F & I_{LF} \\ I_{LC} & I_{LF} & 1 \end{bmatrix} \begin{bmatrix} \dot{\Omega}_C \\ \dot{\Omega}_F \\ \ddot{l}_C \end{bmatrix} + \begin{bmatrix} -R(\vec{r}_{PH} + m_{leg}\vec{r}_{HC}) \cdot \hat{y} & m_{leg}\vec{r}_{HF} \times \vec{r}_{PH} \\ -m_{leg}(\vec{r}_{HF} \times \vec{r}_{PH} + R\vec{r}_{HF} \cdot \hat{y}) & 0 \\ -(\vec{r}_{PH} + m_{leg}\vec{r}_{HC}) \cdot \hat{x}_C + R\cos\theta_C & -m_{leg}\vec{r}_{HF} \cdot \hat{x}_C \end{bmatrix} \begin{bmatrix} \Omega_C^2 \\ \Omega_F^2 \end{bmatrix}$$

$$= \begin{bmatrix} -(\vec{r}_{PH} + m_{leg}\vec{r}_{HC}) \cdot \hat{x}_C \\ -m_{leg}\vec{r}_{HF} \cdot \hat{x}_C \\ 0 \end{bmatrix} 2\dot{l}_C\Omega_C + \begin{bmatrix} (\vec{r}_{PH} + m_{leg}\vec{r}_{HC}) \times \vec{g} \\ m_{leg}\vec{r}_{HF} \times \vec{g} \\ \hat{x}_C \cdot \vec{g} \end{bmatrix} + \begin{bmatrix} T_{hip} \\ -T_{hip} \\ F_{leg} \end{bmatrix}, \tag{50}$$

with F_{leg} given by (17).

References

Alexander, R. McN. 1983 *Animal mechanics*, 2nd edn. Oxford: Blackwell Scientific.

Alexander, R. McN. 1988 *Elastic mechanisms in animal movement*. Cambridge University Press.

Bryson, A. E. & Ho, Y-C. 1975 *Applied optimal control*, 2nd edn. New York: Halsted Press.

Hoerner, S. F. 1965 *Fluid dynamic drag*. Brick Town, New Jersey: Hoerner Fluid Dynamics.

Ker, R. F., Bennett, M. B., Bibby, S. R., Kester, R. C. & Alexander, R. McN. 1987 The spring in the arch of the human foot. *Nature, Lond.* **325**, 147–149.

Margaria, R. 1976 *Biomechanics and energetics of muscular exercise*. Oxford University Press.

McGeer, T. 1988 *Stability and control of two-dimensional biped walking*. CSS-IS TR 88-01. Burnaby, British Columbia: Simon Fraser University, Centre for Systems Science.

McGeer, T. 1989 *Passive bipedal running*. CSS-IS TR 89-02. Burnaby, British Columbia: Simon Fraser University, Centre for Systems Science.

McGeer, T. 1990*a* Passive dynamic walking. *Int. J. robotics Res.* (In the press.)

McGeer, T. 1990*b* Passive walking with knees. *Proceedings of the IEEE International conference on robotics and automation*, May 13–18, 1990. Cincinatti, U.S.A.

McMahon, T. A., Valiant, G. & Frederick, E. C. 1987 Groucho running. *J. appl. Physiol.* **62**, 2326–2337.

Miura, H. & Shimoyama, I. 1984 Dynamic walking of a biped. *Int. J. robotics Res.* (2) **3**, 60–74.

Mochon, S. & McMahon, T. 1980 Ballistic walking: an improved model. *Math. Biosci.* **52**, 241–260.

Raibert, M. H., Brown, H. B. & Chepponis, M. 1984 Experiments in balance with a 3D one-legged hopping machine. *Int. J. robotics Res.* (2) **3**, 75–92.

Raibert, M. H. 1986 *Legged robots that balance.* Cambridge, Massachusetts: MIT Press.

Thompson, C. M. & Raibert, M. H. 1990 Passive dynamic running. In *International symposium of experimental robotics* (ed. V. Hayward & O. Khatib). New York: Springer-Verlag.